

Local-field-correction effects on the electron response functions and on the electrical conductivity in a hydrogen plasma

K. Bennadji*

*Université Paris-Sud, Laboratoire de Physique des Gaz et des Plasmas, UMR8578, Orsay F-91405, France
and Laboratoire d'Electronique Quantique, Faculté de Physique, Université des Sciences et de la Technologie Houari Boumediène (USTHB), El Alia, Boîte Postale 32 Bab Ezzouar 16111, Algiers, Algeria*

M.-M. Gombert

*CNRS, Orsay F-91405, France
and Université Paris-Sud, Laboratoire de Physique des Gaz et des Plasmas, UMR8578, Orsay F-91405, France*

A. Bendib

*Laboratoire d'Electronique Quantique, Faculté de Physique, Université des Sciences et de la Technologie Houari Boumediène (USTHB),
El Alia, Boîte Postale 32 Bab Ezzouar 16111, Algiers, Algeria*

(Received 25 July 2008; revised manuscript received 5 December 2008; published 22 January 2009)

In a one-component plasma constituted by electrons with a uniform positive background, the correlations are studied in the framework of the Singwi, Tosi, Land, and Sjölander (STLS) model. The local-field corrections (LFCs) are calculated with electron density ranging from 10^{19} to 10^{26} cm^{-3} and with a temperature of 10^4 K. Then, a dielectric formalism is used to deduce the potential energy of a positive test charge (a proton) imbedded in the electron medium. A significant departure of this potential from the random phase approximation (RPA) one has been found. In particular, as the density increases, the discrepancy between the two potentials grows up to reach a maximum correlated to the maximum of the electron coupling parameter. In addition, it is found that in both high and low density limits, the STLS and RPA approaches yield similar results. On the other hand, the effect of the LFC on the electrical conductivity is also estimated in hydrogen plasmas.

DOI: [10.1103/PhysRevE.79.016408](https://doi.org/10.1103/PhysRevE.79.016408)

PACS number(s): 52.27.Gr, 52.25.Fi, 71.27.+a

I. INTRODUCTION

The random phase approximation (RPA) is commonly used in the dielectric formalism. This approximation is a weak coupling theory in which the short-range Coulomb and exchange correlations are not correctly taken into account. This shortcoming appears, for instance, while calculating the radial distribution function, which is positive definite. Indeed, at short separation distances, this function takes negative values instead of positive ones. In order to take the intermediate or the strong couplings into consideration, Singwi, Tosi, Land, and Sjölander (STLS) [1] proposed a formalism, which incorporates them through quantities called local-field corrections (LFCs) or local-field factors. They performed their calculations at zero temperature. Later on, other authors made calculations at arbitrary temperature [2]. This method is based on a numerical solution of a set of equations by iterative scheme. It was very time consuming for computers in the 1970s and 1980s when those calculations were originally done. Only preliminary results were obtained; a complete study of coupled plasma properties such as screening, transport, thermodynamic functions, and ionization lowering evaluated with the STLS method, is still an open problem. The aim of this paper is to carry out such calculations for screening and electrical conductivity.

In the literature several works have been devoted to the LFC effects in plasmas. In particular, Ichimaru and Utsumi

proposed useful fitting formulas for LFCs at zero temperature [3,4], which were used in numerous applications. Chabrier extended Utsumi and Ichimaru fitting formula [4] to finite temperatures [5]; he compared the ion-ion screened potential with LFC effects to the RPA one and to the one evaluated with the density functional theory. He found departure of the STLS potential from the RPA one as the electron coupling parameter in degenerate regime increases. Later on, Potekhin, Chabrier, and Yakovlev implemented this formula in their code to calculate transport coefficients in neutron stars [6] and gave a fitting formula for conductivities. Saumon and Chabrier [7] studied the pressure ionization and the plasma phase transition in hydrogen with the use of the LFC to compute the screened interionic potential. On the other hand, Reinholtz, Redmer, and Nagel incorporated the LFC to their study of the thermodynamic and the transport properties of dense hydrogen plasmas [8].

In the beginning of this study, we consider a one-component plasma constituted by nonrelativistic electrons in a uniform neutralizing background formed by positive ions. The electron degeneracy is arbitrary, i.e., electron distribution is the Fermi-Dirac distribution function. Classical, degenerate, and intermediate situations are covered by this distribution. We focus our study on the LFC effects using the STLS model. It is shown here that LFC effects on the electron polarizability are manifest for high electron coupling parameters as STLS potential reaches a maximum of the departure from the RPA one. For a temperature $T=10^4$ K, this occurs in the vicinity of $n_e=10^{22}$ cm^{-3} corresponding to a

*Corresponding author. kbennadji@hotmail.com

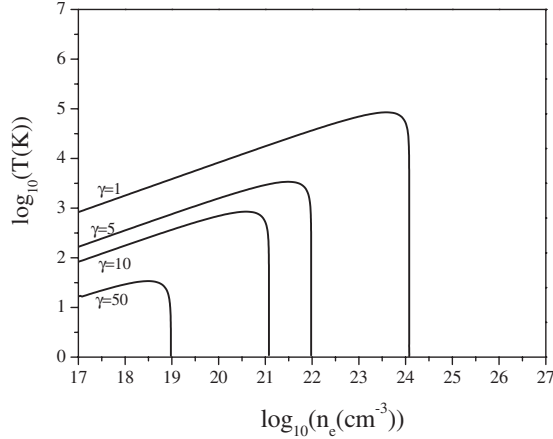


FIG. 1. Coupling parameter lines in the density-temperature plane.

maximum of the coupling parameter. This effect remains negligible at higher or lower densities, which correspond to weak coupling parameters.

The departure of the STLS potential from the RPA one is an important feature, which can considerably change transport properties of plasmas. To emphasize this influence on transport, we have calculated the electrical conductivity for fully ionized hydrogen plasma using a Rousseau-Ziman formula [9–11], which involves a differential cross section combined with the ion-ion structure factor.

The ion-ion structure factor has been computed with the help of the hypernetted chain (HNC) [12] method in a one-component plasma, the plasma made of pointlike ions, the potential between ions being screened by the electrons (STLS or RPA potential) [5]. Thus HNC calculations add the correlations between ions to the ones between electrons. Doing that, we have studied the effects of the correlations between electrons and compared both the models (STLS or RPA) describing the electronic component. Of course, the ionic correlations have been taken into account through the HNC computing. Both differential cross section and ion-ion structure factor are influenced by LFCs (for the electronic component); the latter is decreasing and the former is increasing with the effects of LFCs (or with the electron correlations). The resulting conductivity displays departure from the one obtained if the electrons are treated with the RPA and from other available results [13,6,25].

This paper is organized as follows. The beginning concerns only the one-component plasma. In Sec. II, there are some remarks about the electron coupling parameter. In Sec. III, the STLS model is recalled. Section IV shows numerical results for the LFCs and also for the test charge potential and the electron radial distribution function, taking into account the LFCs or, in the framework of the RPA. In Sec. V, a two-component plasma, a fully ionized hydrogen plasma, is considered. The electrical conductivity has been evaluated and the effects of the LFC in the electron component are studied. Finally, we summarize our results in Sec. VI.

II. COUPLING PARAMETER

In plasma physics, the coupling parameter determines what kind of plasma we deal with. In the special cases of

degenerate and classical plasma, it is given by r_s and Γ , respectively. They are $r_s = a/a_B$ and $\Gamma = e^2/ak_B T$. $a = (3/4\pi n_e)^{1/3}$ is the Wigner-Seitz radius, $a_B = \hbar^2/m_e e^2$ is the Bohr radius, and e is the electron charge. In this study, another parameter is used. It is defined, in arbitrary degeneracy, as follows:

$$\gamma = \frac{e^2/a}{\langle E_c \rangle}, \quad (1)$$

where e^2/a is of the order of magnitude of the mean potential energy per electron and $\langle E_c \rangle$ is the mean kinetic energy per electron,

$$\langle E_c \rangle = 2 \int \frac{d^3k}{(2\pi)^3} \frac{\hbar^2 k^2}{2m_e} f_0(k), \quad (2)$$

m_e is the electron mass, \hbar is the reduced Planck's constant, and k is the wave number associated with the electron momentum. $f_0(k)$ is the Fermi-Dirac distribution function,

$$f_0(k) = \frac{1}{\exp\left(\frac{k^2/k_F^2 - \eta/E_F}{\theta}\right) + 1}, \quad (3)$$

in which $k_F = (3\pi^2 n_e)^{1/3}$ is the Fermi wave number, $\theta = T/T_F$ is the degeneracy parameter, T_F being the Fermi temperature [$T_F = (\hbar^2 k_F^2)/(2m_e k_B)$], where k_B is the Boltzmann constant, and $E_F = k_B T_F$ is the Fermi energy. η is the chemical potential, it is obtained by solving the normalization condition equation

$$3 \int_0^\infty x^2 f_0(k_F x) dx = 1. \quad (4)$$

In the degenerate and classical limits, γ reaches its asymptotic expressions

$$\gamma = \frac{10}{3} \left(\frac{4}{9\pi}\right)^{2/3} r_s \quad \text{for degenerate plasmas } (\theta \ll 1)$$

and

$$\gamma = \frac{2}{3} \Gamma \quad \text{for classical plasmas } (\theta \gg 1). \quad (5)$$

We note that in this work, the numerical results have been evaluated with densities varying from 10^{19} to 10^{26} cm^{-3} and with a fixed temperature of 10^4 K. In these physical situations the corresponding degeneracy parameter varies approximately from the nondegenerate limit $\theta \approx 51$, to the strongly degenerate limit $\theta \approx 10^{-3}$.

In Fig. 1, some curves corresponding to fixed values of γ are drawn in the n - T plane. The area below the $\gamma=1$ curve is the coupled regime area. Figure 2 shows the coupling parameter versus the density at a temperature of 10^4 K. There is a maximum near $n_e = 10^{22}$ cm^{-3} and the classical and degenerate limits are reached for lower and higher densities, respectively.

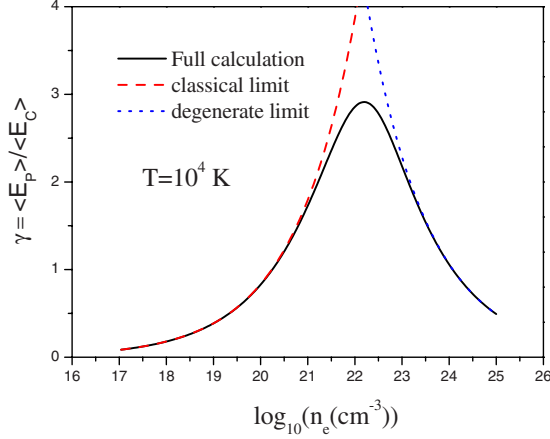


FIG. 2. (Color online) Coupling parameter variations versus density at fixed temperature.

III. LFC IN THE FRAMEWORK OF THE STLS MODEL

Starting from the well-known Bogolyubov-Born-Green-Kirkwood-Yvon (BBGKY) hierarchy, the system of coupled equations for the distribution functions, the STLS theory makes an approximation in the first equation [1]. It is an ansatz that consists of rewriting the two-particle distribution function as follows:

$$f^{(2)}(\vec{r}_1, \vec{r}_2; \vec{p}_1, \vec{p}_2; t) = f(\vec{r}_1, \vec{p}_1, t) f(\vec{r}_2, \vec{p}_2, t) g(|\vec{r}_1 - \vec{r}_2|), \quad (6)$$

where $f^{(2)}$, f , and g are the two-particle distribution function, the one-particle distribution function, and the equilibrium radial distribution function, respectively. Using the fluctuation dissipation theorem, g can be evaluated without the second hierarchy equation, as shown below. By this way, the BBGKY hierarchy is truncated at the first equation. This equation is further used within the linear response formalism to deduce the dielectric response of the electron medium. This is given by the dynamical dielectric function. In the RPA model, the correlations between the plasma electrons, which create the electrical field, are neglected, i.e., in the first equation of the BBGKY hierarchy the function $g(r)$ equals 1. The wave number and frequency-dependent longitudinal dielectric function is [1,2,14]

$$\varepsilon(q, \omega) = 1 - \frac{v(q)\chi^0(q, \omega)}{1 + G(q)v(q)\chi^0(q, \omega)}, \quad (7)$$

where $v(q) = 4\pi e^2/q^2$ is the Fourier transform of the Coulomb potential. $\chi^0(q, \omega)$, the free-particle polarizability (the RPA polarizability), reads

$$\chi^0(q, \omega) = -2 \int \frac{d^3k}{(2\pi)^3} \frac{f_0(\vec{q} + \vec{k}/2) - f_0(\vec{q} - \vec{k}/2)}{\hbar\omega - (E_{\vec{k}+\vec{q}/2} - E_{\vec{k}-\vec{q}/2}) + i\eta}, \quad (8)$$

f_0 being the Fermi-Dirac electron distribution function defined above and $E_{\vec{k}} = \hbar^2 k^2 / 2m_e$, the kinetic energy. η is an infinitesimal. $G(k)$ in Eq. (7) is the LFC, which is introduced

in the STLS model and it reads [1]

$$G(q) = -\frac{1}{n_e} \int \frac{d^3k}{(2\pi)^3} \frac{\vec{q} \cdot \vec{k}}{k^2} [S(|\vec{q} - \vec{k}|) - 1], \quad (9)$$

where $S(q)$ is the static structure factor defined by

$$S(q) = 1 + n_e \int d^3r [g(r) - 1] e^{-i\vec{q} \cdot \vec{r}}. \quad (10)$$

To complete the set of equations, the fluctuation-dissipation theorem [14] is used to write $S(q)$ with respect to $\varepsilon(q, \omega)$,

$$S(q) = -\frac{\hbar q^2}{4\pi^2 e^2 n_e} \int_0^\infty \coth\left(\frac{\hbar\omega}{2k_B T}\right) \text{Im} \left[\frac{1}{\varepsilon(q, \omega)} \right] d\omega. \quad (11)$$

Equations (7), (9), and (11) form a set of closed equations, which has to be self-consistently solved. The method consists first of the choice of a primary LFC (this can be achieved by the trivial value zero or a closer function to the desired solution if it exists). Then, this function is injected in Eq. (7) to evaluate the dielectric function. This one is used in Eq. (11) to calculate the static structure factor, which is used to calculate a new LFC by means of Eq. (9). The process is repeated until a convergent solution is reached. We point out that, making $G=0$ in Eq. (7), the RPA expression for the dielectric function

$$\varepsilon_{RPA}(q, \omega) = 1 - v(q)\chi^0(q, \omega) \quad (12)$$

is reproduced, as expected. Using this last equation, relations (11) and (10) allow one to deduce S_{RPA} and g_{RPA} , respectively. The RPA pair distribution function is negative at short distances, say smaller than a value r_0 . As the density increases, r_0 tends to zero. That is consistent with the validity of the RPA at high densities. On the other hand, the RPA limit also reproduces the Debye screening at low densities. We will see below that the LFCs are not negligible in this regime. As the density decreases, LFC becomes important and paradoxically, the STLS screening tends to the Debye screening.

IV. NUMERICAL RESULTS

In this section, the influence of electron polarization on a test charge embedded in the electron medium is evaluated. More precisely, we have calculated the screened potential produced by a positive ion (proton), the screening being due to the electrons. In an actual plasma made of electrons and ions, the fact that ions move slower than electrons makes the electron response static. This is an approximation (adiabatic approximation), which is not accurate at low densities. The response is given by Eq. (7) in the limit $\omega \rightarrow 0$. Thus

$$\varepsilon(q) = 1 - \frac{v(q)\chi^0(q, 0)}{1 + G(q)v(q)\chi^0(q, 0)}. \quad (13)$$

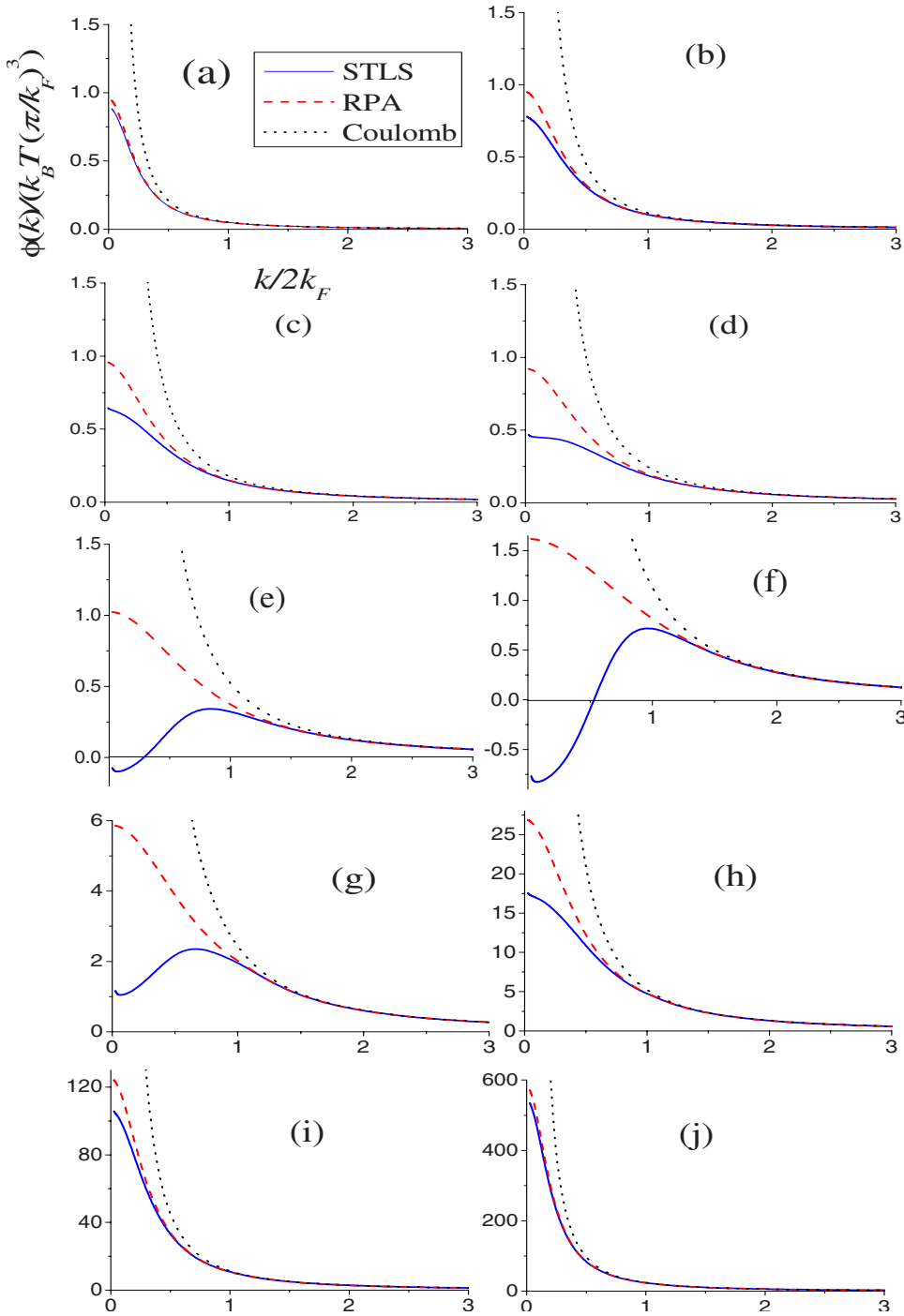


FIG. 3. (Color online) Graphs of potentials in Fourier space with STLS screening, RPA screening, and Coulomb potential at the temperature of 10^4 K. (a) $n_e = 10^{18}$ cm^{-3} , (b) $n_e = 10^{19}$ cm^{-3} , (c) $n_e = 4 \times 10^{19}$ cm^{-3} , (d) $n_e = 10^{20}$ cm^{-3} , (e) $n_e = 10^{21}$ cm^{-3} , (f) $n_e = 10^{22}$ cm^{-3} , (g) $n_e = 10^{23}$ cm^{-3} , (h) $n_e = 10^{24}$ cm^{-3} , (i) $n_e = 10^{25}$ cm^{-3} , and (j) $n_e = 10^{26}$ cm^{-3} .

The ion screened potential is written as follows:

$$\tilde{\phi}(q) = \frac{v(q)}{\varepsilon(q)} \quad \text{and} \quad \phi(r) = \int \frac{d^3q}{(2\pi)^3} \tilde{\phi}(q) e^{-i\vec{q}\cdot\vec{r}}. \quad (14)$$

In Figs. 3(a)–3(j), $\tilde{\phi}(k)$, $\tilde{\phi}_{RPA}(k)$, and $v(k)$ have been plotted for the same temperature of 10^4 K and several densities. The STLS curves are very close to the RPA ones in both high and low density ranges. The departure of the STLS curves from the RPA ones follows exactly the coupling parameter shown in Fig. 2. In particular, a maximum departure is revealed at the density of about $n_e \approx 10^{22}$ cm^{-3} , which corre-

sponds to a maximum coupling parameter. This observation agrees with the one made by Chabrier [5]; he reported an increasing departure of the potential with LFC screening from the one with RPA screening as the degeneracy coupling parameter r_s increases.

Figures 4–6 represent LFCs at low, intermediate, and high densities, respectively. It can be noted that for some low densities, LFCs (Fig. 4) take huge positive and negative values at sufficiently great momentum values. However, those LFCs do not considerably influence the screening. This is because the screening loses its significance at such great momenta, it is only determined by LFCs at small momenta

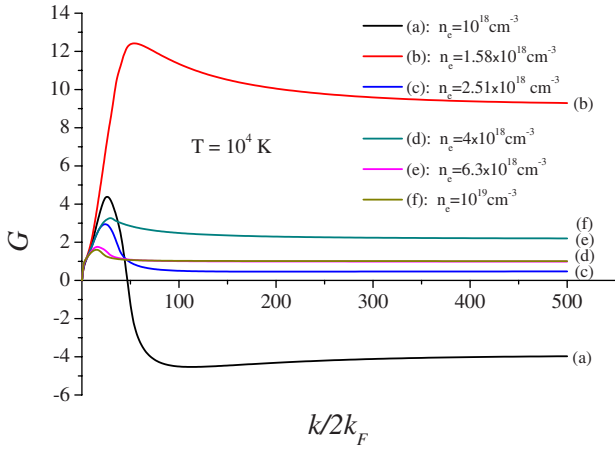


FIG. 4. (Color online) LFCs at low densities.

(say $k/2k_F < 1$). In contrast, the values taken by G in Fig. 5 at long wavelength range make the STLS dielectric function expressed by Eq. (13) negative at small momenta; this means that the inequality $G(q)v(q)\chi^0(q,0) < -1$ is verified in this momentum range. This explains the negative potential values in Figs. 3(e) and 3(f). Remark that the values taken by LFCs, regardless of their effects on relation (13), do not show any peculiar behavior. In Fig. 6, we remark that LFC amplitudes are diminishing with growing density. This is consistent with the fact that RPA is valid at high densities.

Those LFCs considerably correct the negative values of the RPA radial distribution function as can be seen in Figs. 7 and 8. We remark that the STLS radial distribution function in Fig. 7 still has some negative values and that the one in Fig. 8 is entirely positive. This behavior is found in previous works [1,2]; negative values of $g(r)$ appear at high r_s parameters ($r_s > 3.6$) [2]. The STLS formalism is valid at moderate and high densities, as expected, but it still has some shortcomings at low densities. This may come from the ansatz (6) and the truncation of BBGKY hierarchy; this is not entirely correct. Dynamical effects may play a role in this range of densities, thus dynamical LFCs should resolve this problem.

In Fig. 9, $\phi(r)$, $\phi_{RPA}(r)$, and $v(r)$ at the density of 10^{22} cm^{-3} have been represented. The STLS curve presents

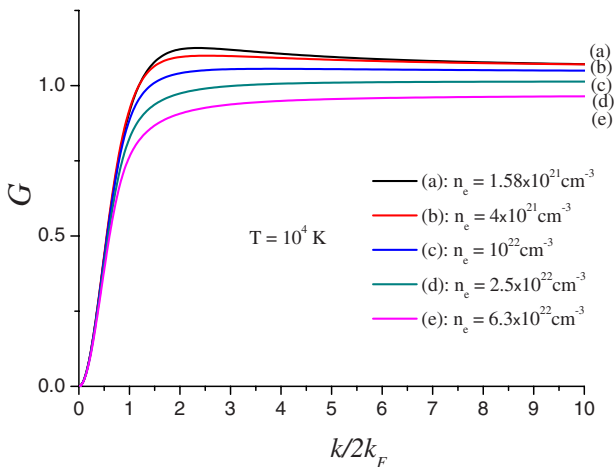


FIG. 5. (Color online) LFCs in the vicinity of the maximum coupling parameter.

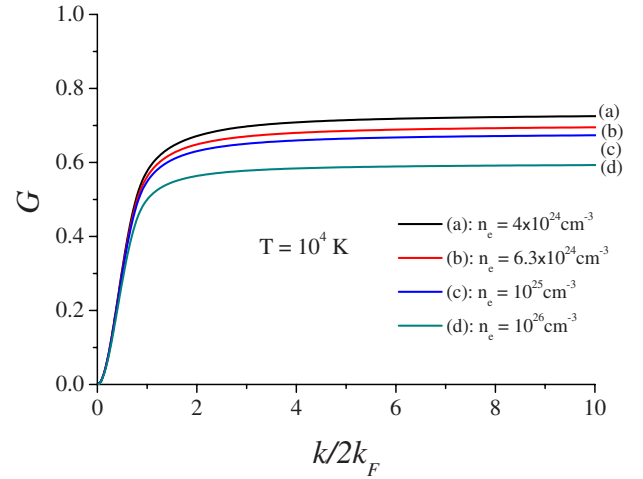
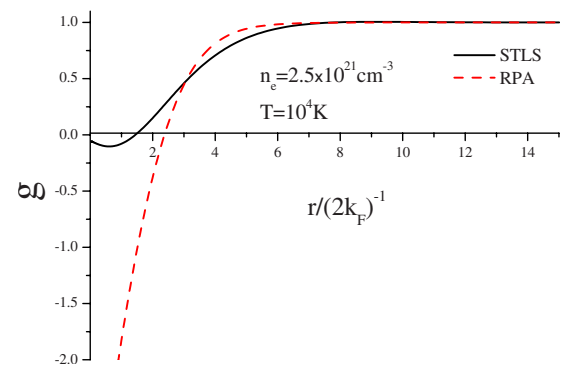


FIG. 6. (Color online) LFCs at high densities.

damped oscillations around zero, which resemble Friedel ones. This effect of LFCs, which produces oscillations in the potential curve, is revealed in Refs. [5,7,8]. Those oscillations are of great importance in transport phenomena and thermodynamics. The differential cross section evaluated with STLS potential is expected to be smaller than the one obtained with the RPA. Actually, while the electron crosses the potential barrier, its quantum phase shift decreases and increases alternatively; the resulting cross section [cf. Eq. (16)] is less than the RPA one. On the other hand, potential in Fig. 9 possesses an attractive branch in the first oscillation, which is the most pronounced one. This is also the case of all potentials in the density range $\Delta n_e = [4 \times 10^{20} \text{ cm}^{-3}, 2.5 \times 10^{23} \text{ cm}^{-3}]$. Some authors think that this attractive behavior gives rise to a plasma phase transition [15–20]. This is still hypothetical. This situation could look like the phase transition in a medium made of neutral gas, which is caused by the attractive branch of the Lenard-Jones potential [21]. It is interesting to remark that instabilities described in Refs. [15–17] occur inside the range Δn_e defined above.

V. ELECTRICAL CONDUCTIVITY OF FULLY IONIZED HYDROGEN PLASMA

Consider now a fully ionized hydrogen plasma. In the following calculations, the electrons constitute a polarizable


 FIG. 7. (Color online) Radial distribution functions at the density of $n_e = 2.5 \times 10^{21} \text{ cm}^{-3}$. The STLS model corrects negative RPA values but slight negative values at short distances still remain.

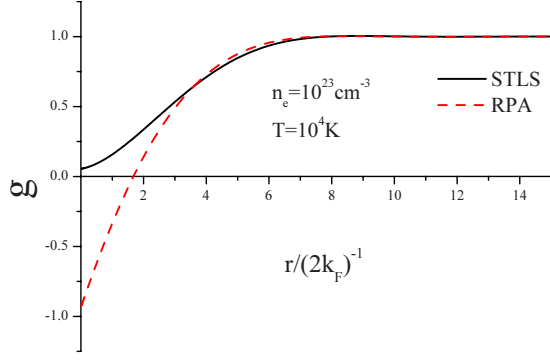


FIG. 8. (Color online) Radial distribution functions at the density of $n_e = 10^{23} \text{ cm}^{-3}$. All STLS values are positive.

medium involving LFC. They screen ions and the resulting ion potential produces all the features described above. The electrical conductivity has been computed, in the same density range and at the same temperature as above. To do so, we have used the Rousseau-Ziman formula [9–11], which correctly accounts for coupling in plasmas. This formula was originally derived from the inverse transport coefficients formula of Edwards [22,23]; it was introduced for liquid metals and was used for coupled plasmas [11]. The electrical resistivity is

$$\rho = -\frac{\hbar}{3\pi Z^2 e^2 n_i} \int_0^\infty dk \frac{\partial f_0}{\partial k} \int_0^{2k} dq q^3 \sigma_k(q) S_{ii}(q), \quad (15)$$

in which Z and n_i are the ion charge and density, respectively (in our case $Z=1$ and $n_i=n_e$), k being the electron momentum and $q=k\sqrt{2[1-\cos(\theta)]}$ —the momentum transferred to ions when the electron emerges at angle θ with the incident direction— f_0 is the electron Fermi-Dirac distribution function, and S_{ii} is the ion-ion structure factor. $\sigma_k(q)$ is the quantum differential cross section [24], which reads

$$\sigma_k(q) = \frac{1}{k^2} \left| \sum_{l=0}^{\infty} (2l+1) e^{i\delta_l} \sin(\delta_l) P_l(\cos(\theta)) \right|^2. \quad (16)$$

l is the electron orbital momentum number, δ_l is the wave phase shift, and P_l is the Legendre polynomial. The phase

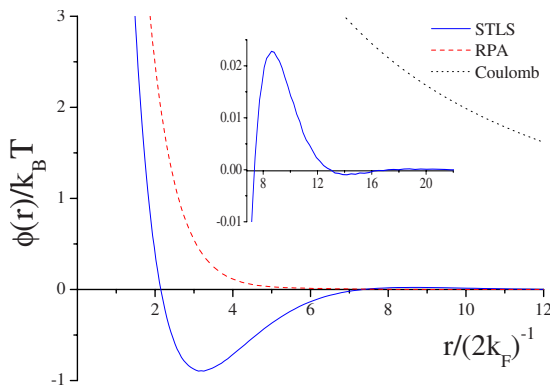


FIG. 9. (Color online) STLS, RPA, and Coulomb potentials in position space at $n_e = 10^{22} \text{ cm}^{-3}$ and $T = 10^4 \text{ K}$. The STLS potential makes damped oscillations around zero (the graph and the panel).

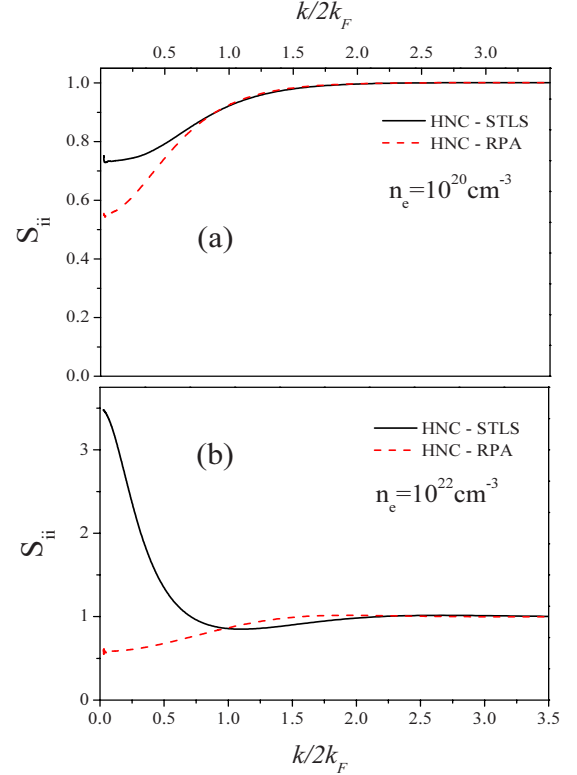


FIG. 10. (Color online) Ion-ion structure factor versus momentum calculated with the HNC scheme at a temperature of 10^4 K . (a) $n_e = 10^{20} \text{ cm}^{-3}$. (b) $n_e = 10^{22} \text{ cm}^{-3}$.

shift is determined by resolving numerically the Schrödinger equation for electron wave function in the field of ion screened potential (STLS or RPA). The ion-ion structure factor S_{ii} is obtained by Fourier transform, from the radial distribution function. The latter, g_{ii} , is obtained by solving numerically the HNC equation for a system of ions interacting via screened potentials (STLS or RPA ones) [5], which is

$$g_{ii}(r) = \exp \left[-\frac{\phi(r)}{k_B T} + n_i \int d^3 r' [g_{ii}(|\vec{r} - \vec{r}'|) - 1] \times \left(g_{ii}(r') - 1 - \ln(g_{ii}(r')) - \frac{\phi(r')}{k_B T} \right) \right]. \quad (17)$$

Here, the HNC calculations do not take into account the “bridge graph” contributions. This fact does not considerably affect values calculated in intermediate and low densities, since the ion-ion coupling parameter is not important in this range of density and ions are strongly screened by electrons. At high densities, the screening length becomes important as well as the ion coupling parameter, thus we expect discrepancies with values calculated with more accurate methods as Monte Carlo simulation. We have focused our attention on the effects of the STLS potential only due to the electrons and evaluated in the previous section. Figure 10 compares S_{ii} calculated with the STLS and RPA potentials. We note that LFCs increase S_{ii} ; they tend to make ions uncorrelated as in Fig. 10(a) or attractive ($S_{ii} > 1$) as in Fig. 10(b). This figure

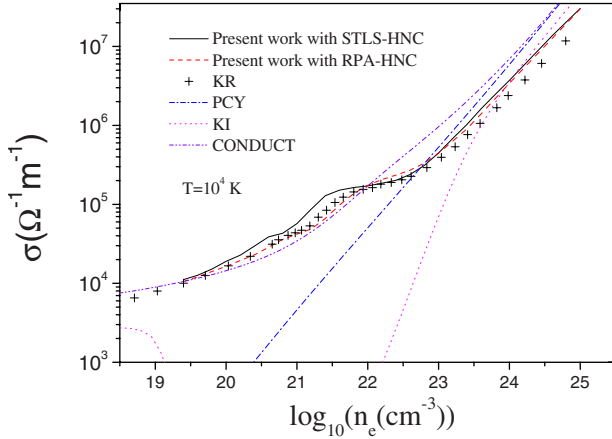


FIG. 11. (Color online) Electrical conductivity of the fully ionized hydrogen plasma. STLS and RPA conductivities are computed with the Rousseau-Ziman formula, S_{ii} being calculated by HNC. A comparison between the STLS model, the RPA model, the KR, PCY, KI and CONDUCT results. Electron-electron collisions are not included in the KR curve and the KI curve passes by a minimum at $n_e = 3.16 \times 10^{20} \text{ cm}^{-3}$ and $\sigma = 12.8 \text{ } \Omega^{-1} \text{ m}^{-1}$ (out of the figure).

shows three phases of ion system if LFCs are taken into account; attractive phase, repulsive phase, and uncorrelated phase. This can be deduced from the potential [Fig. 3(f)].

In Fig. 11, the electrical conductivity [relation (15)] has been plotted with the STLS and RPA models. For comparison, results calculated by Kuhlbrodt and Redmer (KR) [13], by Potekhin, Chabrier, and Yakovlev (PCY) [6], by Kitamura and Ichimaru (KI) [25], and by the code of Potekhin (CONDUCT) [26] have been reported in the same figure. KR used a Zubarev formulation of transport coefficients [13]. Their calculations include electron-electron collisions but neglect ion correlations ($S_{ii}=1$). PCY's curve is produced from a fit that includes LFC in the electron response and relativistic effects [6]. It shows a great discrepancy with respect to our results at low densities and a small difference at high densities. The discrepancy at high density could be due to the computation of the ion-ion structure factor performed with the HNC method in the present work and with the Monte Carlo method in PCY's work. The result given by the code CONDUCT joins PCY's curve at high density and the Spitzer values at low density but does not reproduce features related to electron correlations at intermediate densities. The KI curve is evaluated from a fit [25] that incorporates LFCs of a two-component plasma [27]. At high degeneracy, there are less discrepancies between KI and STLS curves than between PCY and STLS ones. It decreases rapidly at lower degeneracy, passes by a minimum, and increases to reach Spitzer values at classical regime. The KI model takes into account the bound state formation [27]. This explains the sharp decrease and the minimum in Fig. 11.

In the case of uncorrelated ions ($S_{ii}=1$), formula (15) simplifies considerably; the integration on the q variable can be performed analytically and this leads to the well-known standard momentum transport cross section. The resistivity becomes

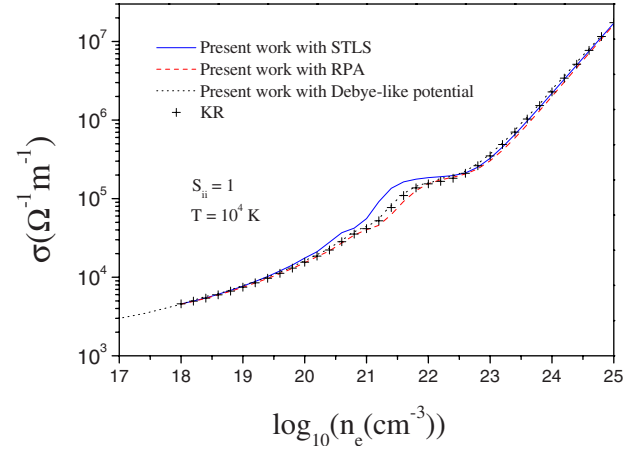


FIG. 12. (Color online) Electrical conductivity of fully ionized hydrogen for uncorrelated ions ($S_{ii}=1$). Comparison between STLS, RPA, Debye-like, and KR.

$$\rho_0 = -\frac{4\hbar}{3\pi Z^2 e^2 n_i} \int_0^\infty dk \frac{\partial f_0}{\partial k} k^2 \sum_{l=0}^\infty (l+1) \sin^2(\delta_{l+1} - \delta_l). \quad (18)$$

The potential used by KR is a Debye-like potential at arbitrary degeneracy [13]. This is a potential expressed as a Debye potential but the screening length is given by means of a Fermi integral, thus it takes into account the degeneracy. It reproduces the Debye potential in the classical limit and the Thomas-Fermi potential in the highly degenerate case. When this potential is used in formula (18), the KR results are reproduced exactly as can be seen in Fig. 12. We point out that KR used a direct formula of the conductivity and our results are deduced from the inverse formula derived by Edwards [22]. The result in Fig. 12 shows the equivalence of the two methods.

In Fig. 11, the STLS conductivity is sometimes greater and sometimes smaller than the RPA one, the reason being that LFC effects act oppositely on cross section and on structure factor, they decrease the former and increase the latter. However, the values taken by the STLS curve in Fig. 12 are always greater than the RPA ones. This is because the structure factor is not taken into account. We point out that the difference of magnitude between the two graphs STLS and RPA in both cases reaches 90% for some densities. This fact gives more importance to electron correlations (LFC) in transport phenomena.

VI. CONCLUSION

We have calculated the LFC in a wide density range and a temperature of 10^4 K in a one-component plasma made of electrons. We have deduced the screened potential of a positive ion (test charge); we have found a significant departure of this potential from the RPA one. This departure follows exactly the electron coupling parameter variations. Especially, a maximum departure is established at the maximum of the coupling parameter. We have also found that the po-

tential calculated in the position space, for the density corresponding to the maximum coupling, presents damped oscillations around zero. We conclude that the electron coupling parameter is a good indicator of the LFC effect on screening. We have also calculated the electrical conductivity of fully

ionized hydrogen with LFC effects. We have found a departure of these values from the RPA ones, which could reach 90% for some densities. We conclude that the electron coupling, here described with the use of the STLS formalism, is important in transport phenomena.

-
- [1] K. S. Singwi, M. P. Tosi, R. H. Land, and A. Sjölander, *Phys. Rev.* **176**, 589 (1968).
- [2] S. Tanaka and S. Ichimaru, *J. Phys. Soc. Jpn.* **55**, 2278 (1986).
- [3] S. Ichimaru and K. Utsumi, *Phys. Rev. B* **24**, 7385 (1981).
- [4] K. Utsumi and S. Ichimaru, *Phys. Rev. A* **26**, 603 (1982).
- [5] G. Chabrier, *J. Phys. (France)* **51**, 1607 (1990).
- [6] A. Y. Potekhin, G. Chabrier, and D. G. Yakovlev, *Astron. Astrophys.* **323**, 415 (1997).
- [7] D. Saumon and G. Chabrier, *Phys. Rev. A* **46**, 2084 (1992).
- [8] H. Reinholz, R. Redmer, and S. Nagel, *Phys. Rev. E* **52**, 5368 (1995).
- [9] J. S. Rousseau, J. C. Stoddart, and N. H. March, *J. Phys. C* **5**, L175 (1972); J. S. Rousseau, J. C. Stoddart, and N. H. March, in *The Properties of Liquid Metals*, edited by S. Takeuchi (Taylor and Francis, London, 1973), p. 249.
- [10] R. Evens, B. L. Gyroffy, N. Szabo, and J. M. Ziman, in *The Properties of Liquid Metals*, edited by S. Takeuchi (Taylor and Francis, London, 1973), p. 319.
- [11] F. Perrot and M. W. C. Dharma-wardana, *Phys. Rev. A* **36**, 238 (1987).
- [12] J.-P. Hansen and I. R. McDonald, *Theory of Simple Liquids* (Academic, London, 1976).
- [13] S. Kuhlbrodt and R. Redmer, *Phys. Rev. E* **62**, 7191 (2000).
- [14] S. Ichimaru, *Statistical Plasma Physics* (Addison-Wesley, Reading, 1994), Vol. II.
- [15] V. S. Filinov *et al.*, *Contrib. Plasma Phys.* **44**, 388 (2004).
- [16] V. S. Filinov *et al.*, *Contrib. Plasma Phys.* **45**, 258 (2005).
- [17] V. S. Filinov, V. E. Fortov, M. Bonitz, and P. R. Levashov, *JETP Lett.* **74**, 384 (2001).
- [18] V. S. Filinov, M. Bonitz, and V. E. Fortov, *JETP Lett.* **72**, 245 (2000).
- [19] B. Holst, R. Redmer, and M. P. Desjarlais, *Phys. Rev. B* **77**, 184201 (2008).
- [20] B. Holst, N. Nettelmann, and R. Redmer, *Contrib. Plasma Phys.* **47**, 368 (2007).
- [21] W. Greiner, L. Neise, and H. Stöcker, *Thermodynamique et Mécanique Statistique* (Springer-Verlag, Berlin, 1999).
- [22] S. F. Edwards, *Proc. Phys. Soc. London* **86**, 977 (1965).
- [23] H. B. Ghassib, R. Gilbert, and G. J. Morgan, *J. Phys. C* **6**, 1841 (1973).
- [24] A. Messiah, *Mécanique Quantique* (Dunod, Paris, 1962), Vol. 1; L. I. Schiff, *Quantum Mechanics* (McGraw-Hill, New York, 1968).
- [25] H. Kitamura and S. Ichimaru, *Phys. Rev. E* **51**, 6004 (1995).
- [26] Conductivity calculated with FORTRAN source code from <http://www.ioffe.ru/astro/conduct/>
- [27] S. Tanaka, X.-Z. Yan, and S. Ichimaru, *Phys. Rev. A* **41**, 5616 (1990).